Journal of Medicinal Chemistry Article

*J. Med. Chem.* **2010,** *53,* 1261–1269 **1261**
DOI: 10.1021/jm901542q

# Novel Highly Potent and Selective $\sigma_1$ Receptor Antagonists Related to Spipethiane

Alessandro Piergentili,[†] Consuelo Amantini,[‡] Fabio Del Bello,[†] Mario Giannella,[†] Laura Mattioli,[‡] Maura Palmery,[§] Marina Perfumi,[‡] Maria Pigini,[†] Giorgio Santoni,[‡] Paolo Tucci,[∥] Margherita Zotti,[∥] and Wilma Quaglia*[,†]

[†]*Dipartimento di Scienze Chimiche, Università di Camerino, via S. Agostino 1, 62032 Camerino, Italy,* [‡]*Dipartimento di Medicina Sperimentale e Sanità Pubblica, Università di Camerino, via Madonna delle Carceri 3, 62032 Camerino, Italy,* [§]*Dipartimento di Fisiologia e Farmacologia Vittorio Erspamer, Università La Sapienza, P.le A. Moro 5, 00185 Roma, Italy, and* [∥]*Dipartimento di Scienze Biomediche, Università di Foggia, via Pinto 1, 71100 Foggia, Italy*

*Received October 17, 2009*

Conservative chemical modifications of the core structure of the lead spipethiane (**1**) afforded novel potent $\sigma_1$ ligands. $\sigma_1$ affinity and $\sigma_1/\sigma_2$ selectivity proved to be favored by the introduction of polar functions (oxygen atom or carbonyl group) in position 3 or 4 (**4**−**6**) or by the elongation of the distance between the two hydrophobic portions of the molecule with the simultaneous presence of a carbonyl group in position 4 (**8** and **9**). The observed cytostatic effect against the human breast cancer cell line MCF-7/ADR, highly expressing $\sigma_1$ receptors, and not against MCF-7, as well as the enhancement of morphine analgesia highlighted the $\sigma_1$ antagonist profile of this series of compounds. In particular, due to its high $\sigma_1$ affinity ($pK_i$ = 10.28) and $\sigma_1/\sigma_2$ selectivity ratio (29510), compound **9** might be a novel valuable tool for $\sigma$ receptor characterization and a suitable template for the rational design of potential therapeutically useful $\sigma_1$ antagonists.

## Introduction

Sigma ($\sigma$) receptors were initially classified as opioid receptor subtypes[1] and subsequently erroneously identified with the phencyclidine (PCP)[a] site on the *N*-methyl-D-aspartate (NMDA) receptor channel.[2] Further studies demonstrated that they were distinct from both opioid receptors and PCP/NMDA receptor complex.[3] At present, $\sigma$ receptors are considered to be a unique receptor family comprising at least two pharmacologically distinct subtypes, namely $\sigma_1$ and $\sigma_2$,[4,5] which are widely distributed in the central nervous system as well as in some peripheral tissues such as digestive tract, kidney, liver, lung, heart, and adrenal medulla.[6,7] They are also present in cells and organs of the immune and endocrine systems.[8] Moreover, both $\sigma$ receptor subtypes are overexpressed in many human and rodent tumor cell lines.[9] While the $\sigma_2$ receptor has not yet been cloned, the $\sigma_1$ subtype has been cloned from various tissues, including guinea pig liver,[10] rat and mouse brain,[11,12] as well as from human placental choriocarcinoma cell lines.[13] Only recently, the hallucinogen *N*,*N*-dimethyltryptamine has been hypothesized to be an endogenous $\sigma_1$ receptor regulator.[14] Although many efforts have been directed to defining the intracellular pathways mediating $\sigma$ receptor signaling (e.g., calcium, $IP_3$, PKC), the molecular mechanisms have not fully been worked out. It remains controversial whether or not sigma receptors are associated with G-proteins.[15,16] Both $\sigma_1$ and $\sigma_2$ receptors are involved in $Ca^{2+}$ release from endoplasmic reticulum and mitochondrial membrane.[17,18] There is evidence suggesting that $\sigma_1$ receptors play a role in the regulation of ion channels including $Ca^{2+}$ and $K^+$ channels[19−21] and are involved in the modulation of glutamatergic,[22] dopaminergic,[23] and cholinergic neurotransmission.[24] Because of their widespread expression in many human tissues and their involvement in several physiological processes, $\sigma$ receptors have proved to be highly attractive pharmacological targets for the treatment of various pathologies. In particular, $\sigma_1$ ligands play a potential role in the treatment of neuropathic pain,[25] depression,[26] cocaine abuse,[27] epilepsy,[28] psychosis,[29] as well as Alzheimer's and Parkinson's disease.[30,31] Moreover, $\sigma_1$ antagonists and $\sigma_2$ agonists may be useful as anticancer agents and radiolabeled ligands as selective tumor imaging agents.[32,33] A variety of structurally unrelated compounds is able to bind $\sigma$ receptors.[34,35] However, while only few $\sigma_2$ ligands generally show a selectivity toward the $\sigma_1$ subtype,[36] several structures are known to bind selectively the $\sigma_1$ receptor and a pharmacophoric model, including an amine site flanked by two hydrophobic domains, has been proposed for $\sigma_1$ ligands.[37] In our previous work about $\sigma$ ligands, the *N*-benzyl-spiropiperidine spipethiane (**1**) proved to be a highly potent and selective $\sigma_1$ ligand.[38] This result and the observation that the bioisosteric replacement of the sulfur atom of **1** with an oxygen atom (compound **2**) (Chart 1) was compatible with the maintenance of the high $\sigma_1$ receptor affinity[38] prompted us to improve our knowledge about structure−affinity and structure−selectivity relationships to better characterize $\sigma$ receptors. Therefore, the methylene analogue **3** was prepared and the bioisosteric substitution with oxygen was extended to position 3 of **1** and **2** (compounds **4** and **5**, respectively).

*To whom correspondence should be addressed. Phone: +390737402237. Fax: +390737637345. E-mail: wilma.quaglia@unicam.it.

[a]Abbreviations: PCP, phencyclidine; NMDA, *N*-methyl-D-aspartate; [$^3$H]DTG, [$^3$H]1,3-di(2-tolyl)guanidine; SRB, sulforhodamine B; $GI_{50}$, growth inhibition 50; PI, propidium iodide; FACS, fluorescence activated cell sorting; 5-HT, 5-hydroxytryptamine; PB28, 1-cyclohexyl-4-[3-(5-methoxy-1,2,3,4,-tetrahydronaphthalen-1-yl)-*n*-propyl]piperazine; MPE, maximum possible effect; $K_i$, inhibition or dissociation constant; PS, phosphatidylserine; TCA, trichloroacetic acid; MFI, mean fluorescence intensity



Published on Web 01/12/2010

Moreover, compound **6** was also included in this study for useful comparison. Compounds **3** and **6** had already been reported in the literature[39,40] but not evaluated for their $\sigma$ binding affinity. Finally, the effect of the elongation of the distance between the two hydrophobic moieties, with a consequent increase of the conformational freedom of the structure, and the oxidation of the methylene group in position 4 (compounds **7**−**10**) were investigated. The pharmacological profiles of the compounds were determined by binding and functional studies.

## Chemistry

Compounds **3**−**5** and the racemic mixtures **7**−**10** were synthesized according to the methods reported in Schemes 1−4. Reduction of 1′-benzyl-1,2,3,4-tetrahydrospiro[naphthalene-2,4′-piperidin]-1-one[41] with borane−dimethyl sulfide complex in dry diglyme afforded the tetraline derivative **3** (Scheme 1). Compounds **4** and **5** were prepared by condensation of (2-mercapto-phenyl)-methanol[42] or commercially available 2-hydroxymethyl-phenol, respectively, with 1-benzoyl-piperidin-4-one, followed by reduction of the amide derivatives **11** and **12** with $LiAlH_4$ (Scheme 2). Treatment of 2-(pyridin-4-yl)-1-benzopyran-4-one[43] with benzyl bromide afforded the intermediate **13**, whose hydrogenation over $PtO_2$ gave compound **8** (Scheme 3). Condensation of 1-(2-mercapto-phenyl)-ethanone[44] or commercially available 1-(2-hydroxy-phenyl)-ethanone with 1-benzyl-piperidine-4-carbaldehyde or 1-phenethyl-piperidine-4-carbaldehyde,[45] respectively, afforded compounds **9** and **10** (Scheme 4). Finally, reduction of **9** with borane-dimethyl sulfide complex in dry diglyme furnished derivative **7** (Scheme 4). Compound **6** was prepared according to the method reported in the literature.[40]

**Chart 1.** Chemical Structures of Spipethiane (**1**) and Its Related Compounds **2**−**10**

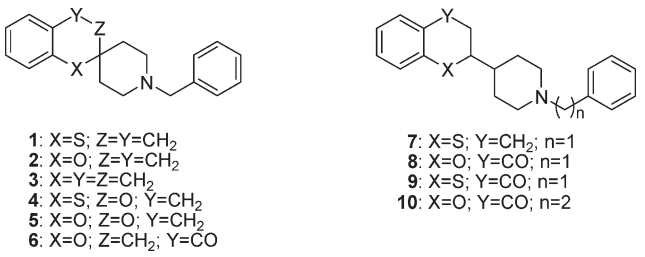


**Scheme 1**[a]

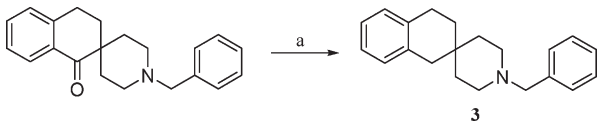


[a] Reagents: (a) $BH_3 \cdot MeSMe$, dry diglyme.

**Scheme 2**[a]

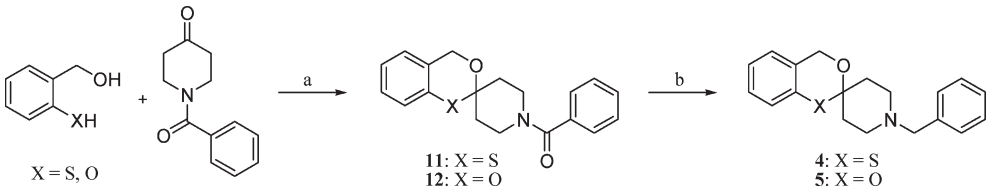


[a] Reagents: (a) HClgas, $CH_2Cl_2$; (b) $LiAlH_4$, THF.

**Scheme 3**[a]

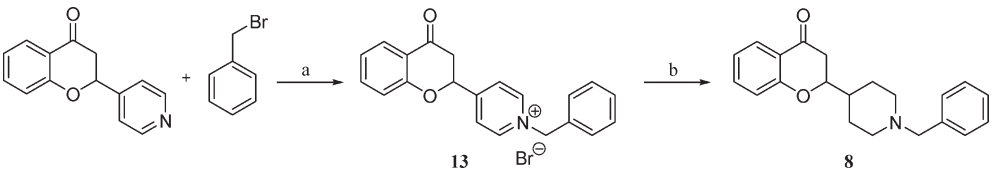


[a] Reagents: (a) Δ, $CH_3CN$; (b) $H_2/PtO_2$, EtOH.

## Biology

**Binding Experiments.** The pharmacological profiles of compounds **3**−**10** were evaluated by radio-receptor binding assays using **1** and haloperidol as reference compounds. [$^3$H](+)-pentazocine and [$^3$H]1,3-di(2-tolyl)guanidine ([$^3$H]DTG) in the presence of 300 nM (+)-pentazocine were used to label $\sigma_1$ and $\sigma_2$ receptors expressed in Jurkat cell and rat cerebral cortex membranes, respectively.[46,47]

## In Vitro Functional Assays

**Cell Growth Inhibition.** The effects of the novel compounds **4**−**10** and **1** on cell growth inhibition were evaluated on MCF-7 and MCF-7/ADR human breast cancer cell lines.[48] These cell lines are characterized by low and high $\sigma_1$ expression, respectively, and they both express high levels of the $\sigma_2$ subtype. The in vitro cell growth inhibition was evaluated using the sulforhodamine B (SRB) assay, according to the National Cancer Institute protocol.[49] The results are expressed as growth inhibition 50 ($GI_{50}$), representing the molar concentration of the compound, which inhibited 50% net of cell growth. Each quoted value is the mean of triplicate experiments.

**Annexin V Staining.** The phosphatidylserine (PS) exposure on MCF-7 and MCF-7/ADR, treated for 48 h with 10 $\mu$M of the selected compounds **1**, **8**, and **9**, was evaluated by Annexin V staining and fluorescence activated cell sorting (FACS) analysis.[50] Data are the percentage of Annexin $V^+$ positive cells ± SEM of three separate experiments.

**Cell Cycle Analysis.** Cell cycle analysis of MCF-7 and MCF-7/ADR, treated for 48 h with 10 $\mu$M of the selected

**Scheme 4**[a]

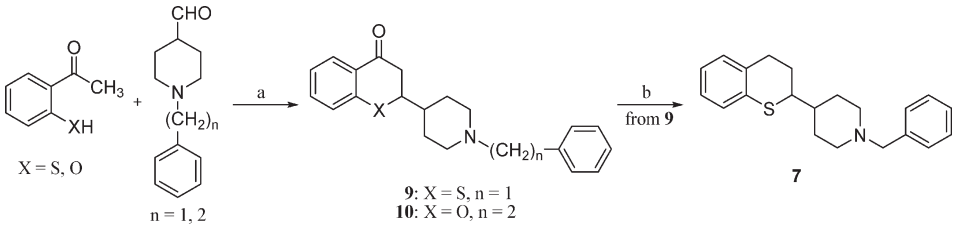


[a] Reagents: (a) pyrrolidine, MeOH; (b) $BH_3 \cdot MeSMe$, dry diglyme.

**Table 1.** Affinity Constants, Expressed as $pK_i$, toward $\sigma_1$ and $\sigma_2$ Receptors,[a] and Efficacy, Expressed as $IC_{50}$, in the Guinea Pig Ileum ($\sigma_2$)[b] for Spipethiane (**1**), and Compounds **2**−**10**

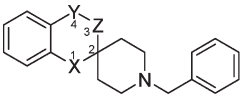


**1**, **3-6**

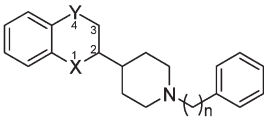


**7-10**

| compd | X | Y | Z | *n* | $pK_i\sigma_1$ | $pK_i\sigma_2$ | $\sigma_1/\sigma_2$[c] selectivity ratio | $IC_{50}$ $\sigma_2$ ($\mu$M) |
|---|---|---|---|---|---|---|---|---|
| **1** (Spipethiane) | S | $CH_2$ | $CH_2$ | | 9.23 | 6.40 | 676 | 6.3 ± 0.92 |
| **2** | O | $CH_2$ | $CH_2$ | | 9.21 | 7.66 | 36 | NT[d] |
| **3** | $CH_2$ | $CH_2$ | $CH_2$ | | 9.36 | 7.85 | 32 | > 10[e] |
| **4** | S | $CH_2$ | O | | 10.05 | 6.65 | 2512 | > 10[e] |
| **5** | O | $CH_2$ | O | | 10.01 | 6.64 | 2344 | 3.9 ± 0.82 |
| **6** | O | CO | $CH_2$ | | 9.68 | 6.52 | 1445 | 7.2 ± 0.62 |
| **7** | S | $CH_2$ | | 1 | 10.24 | 7.24 | 1000 | 8.4 ± 0.54 |
| **8** | O | CO | | 1 | 10.18 | 6.76 | 2630 | 7.5 ± 0.46 |
| **9** | S | CO | | 1 | 10.28 | 5.81 | 29512 | 4.7 ± 0.71 |
| **10** | O | CO | | 2 | 9.96 | 8.08 | 76 | > 10[e] |
| haloperidol | | | | | 8.11 | 6.95 | 15 | NT[d] |

[a] Equilibrium dissociation constants ($K_i$) were derived from $IC_{50}$ values using the Cheng−Prusoff equation.[64] The affinity estimates were derived from displacement of [$^3$H](+)-pentazocine and [$^3$H]DTG in the presence of 300 nM (+)-pentazocine binding for $\sigma_1$ and $\sigma_2$ receptor subtypes, respectively. Each experiment was performed in triplicate. $K_i$ values were from two to three experiments, which agreed within ±10%. [b] $IC_{50}$ represents the half-maximal inhibitory concentration for a drug in a given tissue and was estimated by interpolation from a log−concentration curve which contained 4 concentrations within the range of 20−80% of maximal effect. Values represent the mean ± SEM from six separate experiments. [c] The $\sigma_1/\sigma_2$ selectivity ratio is the antilog of the difference between $pK_i$ at $\sigma_1$ and $\sigma_2$ receptors. [d] Not tested. [e] $IC_{50}$ not obtained up to 10 $\mu$M.

compounds **1**, **8**, and **9**, was evaluated by propidium iodide (PI) staining and FACS analysis.[51] Data are representative of one out of three separate experiments.

**Isolated Guinea Pig Ileum.** Compounds **1** and **3**−**10** were also tested on guinea pig ileum longitudinal muscle/myenteric plexus, where $\sigma$ ligands are known to dose dependently regulate electrically or 5-hydroxytryptamine (5-HT)-evoked contractions.[52]

**In Vivo Study.** $\sigma_1$ antagonists are reported to potentiate opioid analgesia in rats and mice.[53,54] Therefore, the selected compound **9** was evaluated for its ability to modulate morphine analgesia using the classic algesiometric tail flick test.

## Results and Discussion

An analysis of the results reported in Table 1 revealed that all the compounds showed $\sigma_1$ affinity values similar or significantly higher than that of **1**. The $\sigma_2$ affinities were by far lower than those for $\sigma_1$ subtype and ranged within at least 3 orders of magnitude. The bioisosteric replacement of the sulfur atom of **1** by a methylene group, affording **3**, produced the same effect obtained by replacing it with an oxygen atom (compound **2**)[38] (Table 1), a maintenance in $\sigma_1$ affinity, and an increase in that for $\sigma_2$ were obtained with a remarkable decrease of $\sigma_1/\sigma_2$ selectivity ratio. This result allowed us to hypothesize that the sulfur atom in position 1 of **1** does not contribute to $\sigma_1$ receptor binding by means of hydrogen bond formation or electronic effects, as a sulfur, or an oxygen atom, or a methylene group were effective as well. In contrast, these bioisosteric modifications appeared to favor the $\sigma_2$ receptor interaction. A significant increase in $\sigma_1$ affinity and a maintenance in that for $\sigma_2$ subtype with a consequent improved selectivity for $\sigma_1$ subtype were obtained by introducing an oxygen atom in position 3 of **1** and **2** (compounds **4** and **5**, respectively) or by oxidizing the methylene group in position 4 of **2** (compound **6**). The elongation of the distance between the two hydrophobic portions produced a significant increase of $\sigma_1$ affinity and $\sigma_1/\sigma_2$ selectivity (**7** vs **1** and **8** vs **6**). Probably, the improved distance between the two hydrophobic portions, leading to a conformationally more flexible structure, allowed a more productive interaction with $\sigma_1$ receptor sites. More interestingly, such a modification proved to be highly favorable for $\sigma_1$ selectivity when, simultaneously, the methylene group in position 4 of **1** was replaced by a carbonyl function. In fact, the most striking result of the present investigation was the high $\sigma_1$ affinity and selectivity toward $\sigma_2$ receptors displayed by compound **9**; its $\sigma_1/\sigma_2$ selectivity ratio of 29512 was resolutely higher than that observed for the lead **1**. To our knowledge, the highly affine compound **9** is the most selective $\sigma_1$ ligand reported in the literature to date. The further

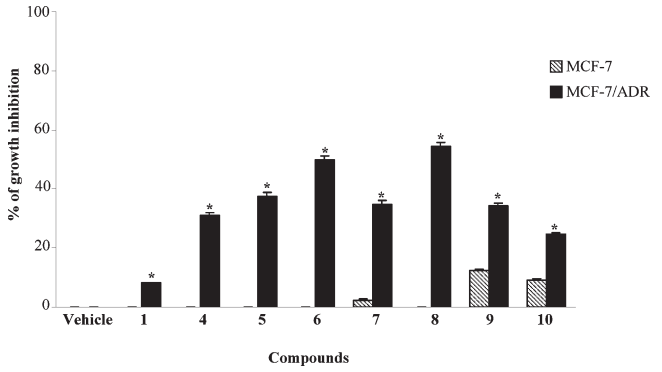


**Figure 1.** Cell growth inhibition of **1**, and compounds **4**−**10** on MCF-7 and MCF-7/ADR cell lines. Cell growth inhibition was evaluated by sulforhodamine B (SRB) assay in MCF-7 and MCF-7/ADR cell lines, treated for 48 h with 10 $\mu$M of $\sigma_1$ receptor compounds. Data are the mean ± SEM of three different experiments. Statistical analysis was performed comparing treated MCF-7 with MCF-7/ADR cells. *$p < 0.01$.

increase of the distance obtained by replacing the *N*-benzyl substituent of **8** by a phenethyl moiety, affording its higher homologue **10**, did not seem to favor the $\sigma_1/\sigma_2$ selectivity ratio because such a modification caused a significant increase in affinity for the $\sigma_2$ subtype. This result confirmed what has previously been reported in the literature for other *N*-benzyl-spiropiperidine analogues,[55] where it has been demonstrated that $\sigma_1$ binding site tolerates groups bulkier and more flexible than the benzyl substituent at the basic nitrogen, but such a modification is especially favorable for $\sigma_2$ binding site.

$\sigma_1$ and $\sigma_2$ receptors are known to be involved in the modulation of cell proliferation and death of MCF-7 and MCF-7/ADR human breast cancer cell lines by inducing cell cycle arrest and apoptosis, respectively.[48] To evaluate the functional behavior of the ligands of the present study, cell growth inhibition induced by lead **1** and derivatives **4**−**10** was determined on these cell lines and their percent inhibition is reported in Figure 1. All compounds specifically inhibited the growth of MCF-7/ADR, the most active being **6** and **8**, with $GI_{50}$ values in a micromolar range order (10.0 and 7.7 $\mu$M, respectively). No significant growth inhibition was observed in low $\sigma_1$ receptor expressing MCF-7. Unlike the $\sigma_2$ agonist and $\sigma_1$ antagonist 1-cyclohexyl-4-[3-(5-methoxy-1,2,3,4,-tetrahydronaphthalen-1-yl)-*n*-propyl]piperazine (PB28), which inhibits the growth of both cell lines,[48] the compounds of the present study showed potent cytostatic effect only against MCF-7/ADR, highly expressing $\sigma_1$ receptors. Therefore, their biological response may be ascribed to a $\sigma_1$ antagonist effect. Several findings indicate that $\sigma_1$ receptor antagonists inhibit cell growth and induce apoptosis.[48,56−58] We initially evaluated the effects of 10 $\mu$M of the lead **1** and of compounds **8** and **9**, selected on the basis of the highest cytostatic activity and $\sigma_1/\sigma_2$ selectivity ratio, respectively, in the cell cycle progression of both MCF-7 and MCF-7/ADR cells. Cell cycle analysis revealed that **8** and **9** increased the number of cells in G0/G1 (30.4% and 27.8%, respectively) and decreased those in S phase (46.4% and 46.7%, respectively), in a $\sigma_1$-dependent manner, as evidenced by the ability of these compounds to selectively affect the high $\sigma_1$ receptor expressing MCF-7/ADR but not the low $\sigma_1$ receptor expressing MCF-7 cells (Figure 2A). Compound **1** did not significantly affect cell cycle in MCF-7/ADR cells, while it slightly increased (16%) the G0/G1 cell number in MCF-7 cells (Figure 2A). A typical feature of apoptotic cell death is the loss of phospholipid asymmetry and the expression of PS on the outer layer of the plasma membrane. We analyzed whether the treatment for 48 h with 10 $\mu$M of compounds **1**, **8**, or **9** induced externalization of PS residues from the inner to the outer leaflet of the plasma membrane in MCF-7 and MCF-7/ADR cancer cells. To this end, MCF-7- and MCF-7/ADR-treated cells were stained with annexin V-FITC and analyzed by flow cytometry.[50] As shown in Figure 2B, the treatment of MCF-7 cells with 10 $\mu$M of compounds **8** and **9** did not induce translocation of PS, whereas PS exposure was observed in MCF-7/ADR cells, although at low levels (10.1% and 12.5%, respectively) with respect to untreated or vehicle-treated cells (data not shown). No Annexin $V^+$ cells were found in both MCF-7 and MCF-7/ADR cells treated with **1**. Our findings indicated that $\sigma_1$ receptor antagonists **8** and **9** inhibited cell growth, arrested cell cycle at G0/G1 phase and induced apoptosis of MCF-7/ADR cells. The potency of **8** and **9**, with respect to **1**, to inhibit cell proliferation correlated with $\sigma_1$ receptor affinity ($pK_i\,\sigma_1$ = 10.18, 10.28, and 9.23, respectively). In addition, the significant differences in the susceptibility of MCF-7 and MCF-7/ADR to $\sigma_1$ receptor-mediated effects observed in our experiments were likely caused by different levels of wild-type $\sigma_1$ receptors expressed in MCF-7 with respect to MCF-7/ADR (MCF7 showed four time less expression of $\sigma_1$ receptors than did MCF7/ADR).[48] The differences in the MCF-7- and MCF-7/ADR-susceptibility to $\sigma_1$ receptor antagonist-mediated effects may also be related to the proliferation status of tumor cells. Because $\sigma_1$ receptor expression positively correlates with the proliferative status of breast cancer cells,[59] and MCF-7/ADR cells show high proliferative status with respect to MCF-7 cells (doubling time 24 h vs 48 h, respectively),[48] the increased sensitivity of MCF-7/ADR, with respect to MCF-7, to **8** and **9** treatment may also depend on the increased proliferation of $\sigma_1$ receptor-positive MCF-7/ADR. However, it cannot be excluded that differences in $\sigma_1$ receptor expression of MCF-7 and MCF-7/ADR, resulting in diverse sensitivity to $\sigma_1$ receptor antagonist-dependent cytostatic effects, may also depend on changes in signal transduction triggering (e.g., rise in $[Ca^{2+}]_i$ levels).[57] Finally, because the $\sigma_1$ receptor antagonists we tested selectively inhibited the growth of MCF-7/ADR cells harboring mutation of p53 tumor suppressor gene, frequently mutated during tumor progression[60] and also involved in the chemotherapeutic drug resistance of breast cancer,[61] we suggest a potential use of these compounds in the therapy of advanced breast cancer. Overall, the consistent accumulation of MCF-7/ADR cancer cells, highly expressing $\sigma_1$ receptors, in G0/G1 phase after $\sigma_1$ receptor antagonists **8** and **9** exposure might be responsible for the $\sigma_1$ receptor-dependent cell growth inhibition and induction of apoptotic cell death.

Data to evaluate the functional activity of all the compounds in the in vitro guinea pig isolated ileum demonstrated that all the derivatives showed $\mu$M $IC_{50}$ values, except for compounds **3**, **4**, and **10**, which failed to inhibit 5-HT-evoked contractions (Table 1). This result along with the observation that all the compounds showed no cytotoxic activity both in MCF-7 and MCF-7/ADR, highly expressing $\sigma_2$ receptors, indicated that they are not $\sigma_2$ agonists.[52]

Previous studies have demonstrated the involvement of $\sigma_1$ receptors in opioid analgesia. Particularly, it has been reported that the $\sigma_1$ selective agonist (+)-pentazocine antagonizes systemic spinal and supraspinal morphine analgesia,[54] while nonselective $\sigma_1$ antagonists, such as haloperidol[62] and

**A**

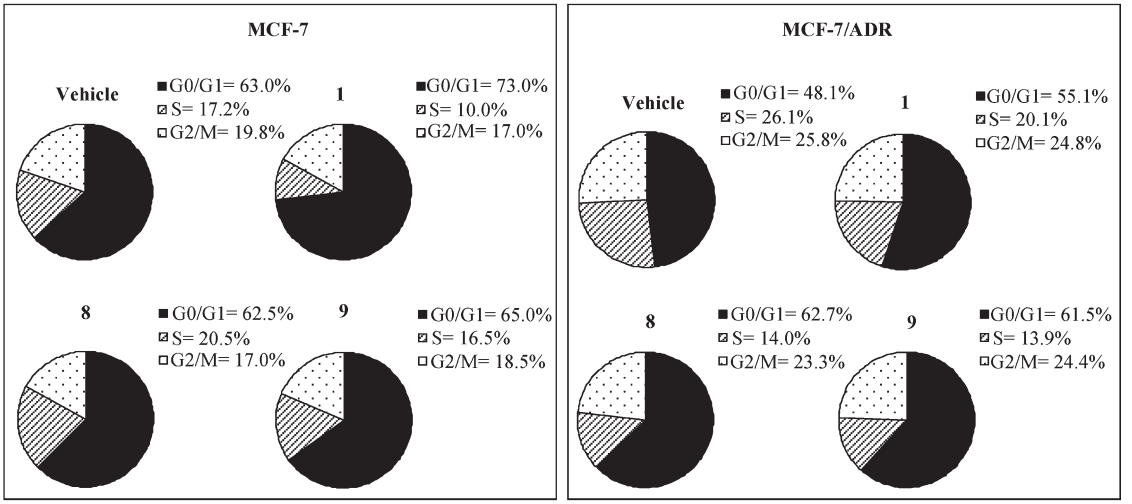


**B**

| Compd. | % Annexin $V^+$ cells | |
|---|---|---|
| | MCF-7 | MCF-7/ADR |
| **Vehicle** | 2.9 ± 0.7 | 3.2 ± 0.9 |
| **1** | 2.7 ± 0.6 | 5.4 ± 0.9* |
| **8** | 3.8 ± 1.0 | 10.1 ± 1.1* |
| **9** | 2.9 ± 0.4 | 12.5 ± 0.9* |

**Figure 2.** (A) Selected compounds induce G0/G1 cell growth arrest. Cell cycle analysis of MCF-7 and MCF-7/ADR, treated with 10 $\mu$M of compounds **1**, **8**, and **9**, was performed by PI staining. Cell percentage relative to different cycle phases are indicated. Data are representative of three different experiments. (B) PS exposure in MCF and MCF-7/ADR. The PS exposure on MCF-7 and MCF-7/ADR, treated for 48 h with 10 $\mu$M of compounds **1**, **8**, and **9**, was evaluated by Annexin V staining and FACS analysis. Data are the percentage of Annexin $V^+$ positive cells ± SEM of three separate experiments. Statistical analysis was performed comparing vehicle treated with selected compound-treated cells. *$p < 0.01$.

structurally related compounds,[53] enhance it in mice and rats. In this study, we provided evidence that compound **9**, selected on the basis of its highest affinity and selectivity for the $\sigma_1$ receptor, was able to induce a significant increase in morphine-induced analgesia. In fact, as shown in Figure 3, **9** had no analgesic effect when given alone but significantly increased the analgesic response induced by morphine at all times, as evidenced by increased reaction latencies expressed as %MPE in the tail flick test. The maximum analgesic effect of morphine (5 mg/kg, sc) was observed after 30 min, and then it progressively decreased. Pretreatment with **9** (1 mg/kg) significantly increased the antinociceptive effect produced by morphine over the entire time course starting at 60 min. The ANOVA confirmed a statistically significant treatment effect [$F(2.20) = 48.545$; $p < 0.001$]. Therefore, according to the literature, our data provided evidence of a $\sigma_1$ antagonist profile of compound **9**.[53,62]

In conclusion, our lead spipethiane (**1**) proved to be a suitable template for the design of novel $\sigma$ ligands. Indeed, conservative chemical modifications of its structure such as (i) the introduction of polar functions (oxygen atom or carbonyl group) in position 3 or 4 (**4**–**6**), or (ii) the elongation of the distance between the two hydrophobic portions of the molecule with the simultaneous presence of a carbonyl group in position 4 (**8** and **9**), provided efficient $\sigma_1$ ligands endowed

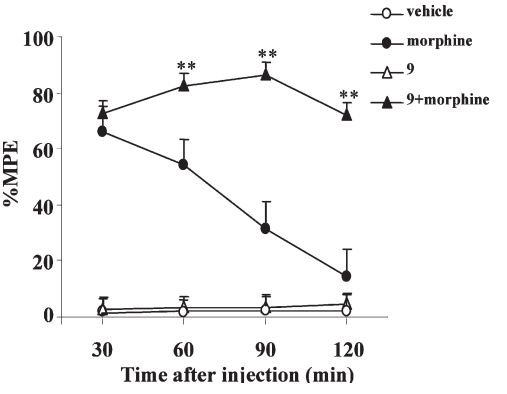


**Figure 3.** Effect of **9** (1 mg/kg, sc) pretreatment on morphine (5 mg/kg, sc) analgesia in the tail flick test. The reaction latencies were expressed as a percent of the maximum possible effect (%MPE). Values are mean ± SEM of 8 mice. **$p < 0.01$ compared to morphine group.

with high $\sigma_1/\sigma_2$ selectivity ratio. To our knowledge, compound **9** is the most selective $\sigma_1$ ligand reported to date ($\sigma_1/\sigma_2$ selectivity ratio = 29510). The observed cytostatic effect only against the human breast cancer cell line MCF-7/ADR, highly expressing $\sigma_1$ receptors, and the enhancement of morphine analgesia highlighted the $\sigma_1$ antagonist profile of this series of compounds. Moreover, from our study it also emerged that the $\sigma_2$ affinity appeared significantly favored by the bioisosteric substitution of the sulfur atom with an oxygen atom or a methylene group (**2** and **3**, respectively) as well as by the replacement of the *N*-benzyl with the *N*-phenethyl substituent and the simultaneous presence of a carbonyl group in position 4 (**10**). These results are the basis for promising future work directed to the characterization of $\sigma$ receptors and to provide potential therapeutical agents.

## Experimental Section

**Chemistry.** Melting points were taken in glass capillary tubes on a Büchi SMP-20 apparatus and are uncorrected. IR and NMR spectra were recorded on Perkin-Elmer 297 and Varian Gemini 200 instruments, respectively. Chemical shifts are reported in parts per million (ppm) relative to tetramethylsilane (TMS), and spin multiplicities are given as s (singlet), d (doublet), dd (double doublet), ddd (doublet of double doublets), t (triplet), q (quartet), or m (multiplet). IR spectral data (not shown because of the lack of unusual features) were obtained for all compounds reported and are consistent with the assigned structures. The microanalyses were performed by the Microanalytical Laboratory of our department. The elemental composition of the compounds agreed to within ±0.4% of the calculated value. Chromatographic separations were performed on silica gel columns (Kieselgel 40, 0.040−0.063 mm, Merck) by flash chromatography. The term "dried" refers to the use of anhydrous sodium sulfate. Compounds were named following IUPAC rules as applied by Beilstein-Institut AutoNom (version 2.1), a software for systematic names in organic chemistry. The purity of the new compounds was determined by combustion analysis and was ≥95%.

**1′-Benzyl-1,2,3,4-tetrahydrospiro[naphthalene-2,4′-piperidine] Oxalate (3).** A solution of 10 M $BH_3 \cdot Me_2S$ (0.52 mL) in dry diglyme (1 mL) was added dropwise at room temperature to a solution of 1′-benzyl-1,2,3,4-tetrahydrospiro[naphthalene-2,4′-piperidin]-1-one[41] (0.55 g, 1.80 mmol) in dry diglyme (10 mL) with stirring under a stream of dry nitrogen with exclusion of moisture. When the addition was completed, the reaction mixture was heated at 120 °C for 8 h. After cooling to 0 °C, excess borane was destroyed by cautious dropwise addition of MeOH (10 mL). The resulting mixture was left to stand at room temperature, cooled to 0 °C, treated with HCl gas for 15 min, then heated to 120 °C for 4 h. Removal of the solvent under reduced pressure gave a residue, which was dissolved in water. The aqueous solution was basified with NaOH pellets and extracted with $CHCl_3$. Removal of dried solvents gave a residue, which was purified by column chromatography. Eluting with cyclohexane/EtOAc (8:2) afforded **3** as the free base: 0.4 g; 76% yield. $^1$H NMR ($CDCl_3$): $\delta$ 1.30−1.75 (m, 6H, 3, 3′ and 5′-$CH_2$), 2.32−2.83 (m, 8H, 1, 4, 2′ and 6′-$CH_2$), 3.52 (s, 2H, $CH_2$Ar), 7.0−7.43 (m, 9H, ArH). The free base was transformed into the oxalate salt, which was recrystallized from EtOH: mp 219−221 °C. Anal. ($C_{21}H_{25}N \cdot C_2H_2O_4 \cdot 0.25H_2O$) C, H, N.

**1′-Benzoyl-spiro[4*H*-3,1-benzoxathiin-2,4′-piperidine] (11).** 1-Benzoyl-piperidin-4-one (2.47 g, 12.13 mmol) was added to an ice-cooled solution of (2-mercapto-phenyl)-methanol[42] (1.7 g, 12.13 mmol) in dry $CH_2Cl_2$ (62 mL). Anhydrous HCl gas was bubbled until saturation, followed by the addition of $Na_2SO_4$ (3 g). After stirring at room temperature for 24 h the solution was filtered, washed with $H_2O$, 2N NaOH, and $H_2O$. Removal of dried solvents gave an oil, which was purified by column chromatography. Eluting with cyclohexane/EtOAc (8:2) afforded **11** as a solid: 2.6 g; 66% yield; mp 84−85 °C. $^1$H NMR ($CDCl_3$): $\delta$ 1.90−2.29 (m, 4H, 3′ and 5′-$CH_2$), 3.44−4.15 (m, 4H, 2′ and 6′-$CH_2$), 4.85 (s, 2H, 4-$CH_2$), 7.04−7.43 (m, 9H, ArH).

**1′-Benzoyl-spiro[4*H*-1,3-benzodioxin-2,4′-piperidine] (12).** This was synthesized from 2-hydroxymethyl-phenol following the procedure described for **11**. Eluting with cyclohexane/EtOAc (7.5:2.5) afforded **12** as an oil: 11% yield. $^1$H NMR ($CDCl_3$): $\delta$ 1.68−2.17 (m, 4H, 3′ and 5′-$CH_2$), 3.36−4.14 (m, 4H, 2′ and 6′-$CH_2$), 4.86 (s, 2H, 4-$CH_2$), 6.83−7.44 (m, 9H, ArH).

**1′-Benzyl-spiro[4*H*-3,1-benzoxathiin-2,4′-piperidine] Oxalate (4).** A solution of **11** (1.0 g; 3.07 mmol) in dry $Et_2O$ (70 mL) was added dropwise to a cooled (0 °C) suspension of $LiAlH_4$ (0.35 g; 9.22 mmol) in dry $Et_2O$ (65 mL). The reaction was left at room temperature for 24 h and then heated to reflux for 5 h. After cooling, $H_2O$ (0.35 mL), 5N NaOH (0.35 mL), and again $H_2O$ (1.75 mL) were sequentially added. After filtration, the solid was washed with ethyl acetate. Removal of dried solvents gave a residue, which was purified by column chromatography. Eluting with cyclohexane/EtOAc (8:2) afforded **4** as the free base: 0.93 g; 97% yield; mp 75−77 °C. $^1$H NMR ($CDCl_3$): $\delta$ 2.12 (m, 4H, 3′ and 5′-$CH_2$), 2.59 (m, 4H, 2′ and 6′-$CH_2$), 3.55 (s, 2H, $CH_2$Ar), 4.83 (s, 2H, 4-$CH_2$), 7.00−7.38 (m, 9H, ArH). The free base was transformed into the oxalate salt, which was recrystallized from EtOH: mp 206−207 °C. Anal. ($C_{19}H_{21}NOS \cdot C_2H_2O_4$) C, H, N, S.

**1′-Benzyl-spiro[4*H*-1,3-benzodioxin-2,4′-piperidine] Oxalate (5).** This was synthesized from **12** following the procedure described for **4**. Eluting with cyclohexane/EtOAc (8.5:1.5) afforded **5** as the free base: 69% yield. $^1$H NMR ($CDCl_3$): $\delta$ 1.97 (m, 4H, 3′ and 5′-$CH_2$), 2.57 (t, $J$ = 8.11 Hz, 4H, 2′ and 6′-$CH_2$), 3.57 (s, 2H, $CH_2$Ar), 4.85 (s, 2H, 4-$CH_2$), 6.83−7.39 (m, 9H, ArH). The free base was transformed into the oxalate salt, which was recrystallized from 2-PrOH: mp 188−189 °C. Anal. ($C_{19}H_{21}NO_2 \cdot C_2H_2O_4$) C, H, N.

**(±)-1-Benzyl-4-(1-benzopyran-4-one-2-yl)pyridinium Bromide (13).** A solution of 2-(pyridin-4-yl)-1-benzopyran-4-one[43] (1.0 g, 4.44 mmol) and benzyl bromide (1.08 mL, 8.88 mmol) in $CH_3CN$ (14 mL) was stirred at reflux for 3 h. After cooling to room temperature, diethyl ether was added and the solid was filtered and crystallized twice from EtOH: 1.2 g; 68% yield; mp 243−245 °C dec. $^1$H NMR ($CD_3OD$): $\delta$ 3.11 (m, 2H, 3-$CH_2$), 5.89 (s, 2H, $CH_2$Ar), 5.99 (dd, $J$ = 7.42, 14.2 Hz, 1H, 2-CH), 7.11−9.20 (m, 13H, ArH).

**(±)-2-(1-Benzyl-piperidin-4-yl)-1-benzopyran-4-one Oxalate (8).** Compound **13** (0.87 g, 2.20 mmol) in EtOH (20 mL) was hydrogenated over $PtO_2$ (0.10 g) at room temperature for 35 min and 30 psi of pressure. The mixture was filtered through celite, and the solvent was removed in vacuo. The residue was treated with 1N NaOH and extracted with EtOAc. Removal of dried solvents gave a residue, which was purified by column chromatography. Eluting with $CHCl_3$/MeOH (9.8:0.2) afforded **8** as the free base: 0.22 g; 31% yield. $^1$H NMR ($CDCl_3$): $\delta$ 1.41−2.12 (m, 7H, 3′ and 5′-$CH_2$, 4′-CH, 2′ and 6′-$CH_{ax}$), 2.70 (m, 2H, 3-$CH_2$), 2.99 (m, 2H, 2′ and 6′-$CH_{eq}$), 3.53 (s, 2H, $CH_2$Ar), 4.24 (dt, $J$ = 8.92, 13.4 Hz, 1H, 2-CH), 6.92−7.92 (m, 9H, ArH). The free base was transformed into the oxalate salt, which was recrystallized from 2-PrOH: mp 195−196 °C. Anal. ($C_{21}H_{23}NO_2 \cdot C_2H_2O_4$) C, H, N.

**(±)-2-(1-Benzyl-piperidin-4-yl)-1-benzothiopyran-4-one Oxalate (9).** A solution of 1-(2-mercapto-phenyl)-ethanone[44] (1.24 g, 8.15 mmol), 1-benzyl-piperidine-4-carbaldehyde (1.66 g, 8.15 mmol), and pyrrolidine (1.16 g, 16.3 mmol) in MeOH (42 mL) was refluxed for 2 h. After cooling, the solvent was evaporated and the residue was dissolved in $NaHCO_3$ saturated solution and extracted with EtOAc. Removal of dried solvents gave a residue, which was purified by column chromatography. Eluting with EtOAc afforded **9** as the free base: 2.0 g; 73% yield; mp 80−82 °C. $^1$H NMR ($CDCl_3$): $\delta$ 1.38−2.02 (m, 7H, 3′,

and 5′-$CH_2$, 4′-CH, 2′ and 6′-$CH_{ax}$), 2.80−3.12 (m, 4H, 3-$CH_2$, 2′ and 6′-$CH_{eq}$), 3.35 (m, 1H, 2-CH), 3.50 (s, 2H, $CH_2Ar$), 7.10−8.11 (m, 9H, ArH). The free base was transformed into the oxalate salt, which was recrystallized from MeOH: mp 218−220 °C. Anal. ($C_{21}H_{23}NOS \cdot C_2H_2O_4$) C, H, N, S.

**(±)-2-(1-Phenethyl-piperidin-4-yl)-1-benzopyran-4-one Oxalate (10).** This was synthesized from 1-(2-hydroxy-phenyl)-ethanone and 1-phenethyl-piperidine-4-carbaldehyde[45] following the procedure described for **9**. Eluting with EtOAc afforded **10** as the free base: 69% yield; mp 96−98 °C. $^1$H NMR ($CDCl_3$): $\delta$ 1.43−2.18 (m, 7H, 3′, and 5′-$CH_2$, 4′-CH, 2′ and 6′-$CH_{ax}$), 2.52−3.20 (m, 8H, 3-$CH_2$, 2′, 6′-$CH_{eq}$ and $NCH_2CH_2Ar$), 4.23 (ddd, $J$ = 8.12, 4.27, 11.11 Hz, 1H, 2-CH), 6.92−7.92 (m, 9H, ArH). The free base was transformed into the oxalate salt, which was recrystallized from EtOH: mp 216−217 °C. Anal. ($C_{22}H_{25}NO_2 \cdot C_2H_2O_4$) C, H, N.

**(±)-4-1-Benzothiopyran-2-yl-1-benzyl-piperidine Oxalate (7).** This was synthesized from **9** following the procedure described for **3**. Eluting with EtOAc afforded **7** as the free base: 56% yield; mp 90−92 °C. $^1$H NMR ($CDCl_3$): $\delta$ 1.32−2.32 (m, 9H, 3, 3′, and 5′-$CH_2$, 4′-CH, 2′ and 6′-$CH_{ax}$), 2.71−3.70 (m, 5H, 2-CH, 4-$CH_2$, 2′ and 6′-$CH_{eq}$), 3.49 (s, 2H, $CH_2Ar$), 6.92−7.40 (m, 9H, ArH). The free base was transformed into the oxalate salt, which was crystallized from EtOH: mp 198−200 °C. Anal. ($C_{21}H_{25}NS \cdot C_2H_2O_4 \cdot 0.5H_2O$) C, H, N, S.

**Biology. Radioligand Binding Assays to $\sigma$ Receptors.** The $\sigma$ binding assays were performed by CEREP (Paris, France) according to Ganapathy et al.[46] for $\sigma_1$ binding and Bowen et al.[47] for $\sigma_2$ binding. In brief, the $\sigma_1$ binding assay was performed by incubating Jurkat cell membranes (100−200 $\mu$g protein per tube) with [$^3$H](+)-pentazocine (8 nM) and a range of concentrations of test compounds, at 22 °C for 2 h, in 5 mM Tris/HCl buffer, pH = 7.4. The $\sigma_2$ binding assay was performed by incubating rat cerebral cortex membranes (100−200 $\mu$g protein per tube) with [$^3$H]DTG (5 nM), in the presence of (+)-pentazocine (300 nM) to saturate $\sigma_1$ sites, and a range of concentrations of test compounds, at 22 °C for 2 h, in 5 mM Tris/HCl buffer, pH = 7.4. The final assay volume was 0.5 mL. Nonspecific binding was defined, in both assays, as that remaining in the presence of 10 $\mu$M haloperidol. The reaction was terminated by rapid filtration through Whatman GF/B filters, which were then washed with 5 × 1 mL ice-cold 0.9% NaCl (saline) solution and allowed to dry before bound radioactivity was measured using liquid scintillation counting. The protein concentration in the homogenates was determined using the method of Bradford.[63]

**Cell Line Culture.** The two breast cancer cell lines of human origin, MCF-7 adriamycin-sensitive (p53 wild-type) and MCF-7/ADR-adriamycin-resistant (p53 mutated), characterized by low and high $\sigma_1$ receptor expression,[48] respectively, were kindly provided by Prof. G. Zupi (IRE, Rome, Italy). The cells were routinely cultured in RPMI 1640 supplemented with 10% FCS, 2 mmol/L-glutamine, 50000 units/L-penicillin, and 80 $\mu$mol/L-streptomycin in a humidified incubator at 37 °C with 5% $CO_2$ atmosphere.

**In Vitro Cytotoxicity Assay.** Human MCF-7 and MCF-7/ADR cell lines were used for cytotoxicity testing in vitro using the SRB (Sulforhodamine B) assay.[49] Cells were maintained as stocks in DMEM (Gibco) supplemented with 10% fetal bovine serum (Gibco), 2 mM L-glutamine (Gibco). Cell cultures were passaged twice weekly using trypsin-EDTA to detach the cells from their culture flasks. The rapidly growing cells were harvested, counted, and seeded under the appropriate concentrations (1 × $10^4$ cells/well) in 96-well microtiter plates. After 24 h, different doses of compound (from 10 nM to 10 $\mu$M) dissolved in culture medium were applied to the culture wells in quadruplicate and incubated for 48 h at 37 °C in a 5% $CO_2$ atmosphere and 95% relative humidity. At the same time, a plate was tested to value the cell population before the drug addition ($T_z$). Culture fixed with cold trichloroacetic acid (TCA) (J. T. Baker B.V., Deventer, Holland) were stained by 0.4% SRB (Sigma-Aldrich, Milan, Italy), dissolved in 1% acetic acid. Bound stain was subsequently solubilized with 10 mM Trizma (Sigma-Aldrich, Milan, Italy), and the absorbance read on the microplate reader Dynatech model MR 700 at a wavelength of 520 nm. The cytotoxic activity was evaluated by measuring the drug concentration resulting in a 50% reduction in the net protein increase (as measured by SRB staining) in control cells during the drug incubation ($GI_{50}$). The percentage of growth inhibition was calculated as: $[(T_i - T_z)/(C - T_z)] \times 100$ for concentration for which $T_i \geq T_z$; $[(T_i - T_z)/T_z] \times 100$ for concentration for which $T_i < T_z$, where $T_z$ = absorbance time zero, $C$ = absorbance in the presence of vehicle, and $T_i$ = absorbance in the presence of drug at different concentrations. $GI_{50}$, determined by software, was obtained by interpolation in a graph % of growth versus Log(M). Each quoted value represents the mean of triplicate.

**Annexin-V Staining.** Phosphatidylserine (PS) exposure on MCF-7 and MCF-7/ADR cells was detected by Annexin V staining and cytofluorimetric analysis.[50] Briefly, 3 × $10^5$/mL MCF-7 and MCF-7/ADR cells were treated with 10 $\mu$M of tested compound for 48 h at 37 °C, 5% $CO_2$, in a 24 well plate. After treatment, cells were stained with Annexin V-FITC (1:40) for 10 min in binding buffer (10 mM Hepes/NaOH, pH 7.4, 140 mM NaCl, 2.5 mM $CaCl_2$) at room temperature, detached from the plate, and washed once with binding buffer. Samples were then analyzed by a FACScan cytofluorimeter using the CellQuest software and data were expressed as mean fluorescence intensity (MFI).

**Cell Cycle Analysis.** First, 3 × $10^5$/mL MCF-7 and MCF-7/ADR cells were grown with compounds **1**, **8**, and **9** (10 $\mu$M) for 48 h at 37 °C and 5% $CO_2$. After washing in PBS, cells were suspended in 1 mL of PBS, fixed by adding 2.5 mL of 70% cold ethanol, and incubated on ice for 15 min. Then cells were centrifuged in order to discard ethanol, stained for 40 min at 37 °C with 0.5 mL of PI solution (50 $\mu$g/mL PI, 0.1 mg/mL RNase A, 0.05% Triton-X-100 in PBS), and finally analyzed by flow cytometry. The percentage of positive cells determined over 10000 events was analyzed on a FACScan cytofluorimeter using the CellQuest software (Becton Dickinson) and the Cyflogic software (Cyflo LTD).

**Guinea Pig Ileum Functional Assays.** The experimental procedure was essentially that previously described.[52] Male guinea pig weighing 300−400 g (Harlan, Italy) were housed four per cage in a room with controlled temperature (22 ± 1 °C) and light (12 h per day) for at least 4 days before being used. Animals were cared for in accordance with the principles and guidelines of the Italian Ethics governing these experiments.

Guinea pigs were killed by a blow on the neck. Three to six segments, 2−3 cm long, of ileum were excised from the same animal, discarding the 10 cm nearest the cecum. The segments were cleaned with Tyrode's solution and set up under 1 g tension in 10 mL organ bath containing Tyrode's solution, maintained at 37 °C, and gassed with 95% $O_2$ and 5% $CO_2$. Changes in tension were recorded under isotonic conditions (1 g) by a transducer connected to a recorder (Ugo Basile, Italy) and calibrated before each experiment.

In experiments, 1 $\mu$M ketanserin was included in the Krebs buffer during the entire experiment. Following the 90 min equilibration period, 3 noncumulative concentration−response curves for 5-hydroxytryptamine (5-HT) were obtained, the first and third in Krebs buffer and the second in Krebs buffer containing a concentration of a test compound. 5-HT was added to each organ bath by microliter syringe and remained in contact with the strips for 1 min. The maximum height of the resulting contraction was recorded for each concentration of 5-HT. An interval of 20 min between 5-HT applications was allowed, during which the strips were washed extensively; preliminary experiments determined that this procedure avoided tachyphylaxis of 5-HT responses. Only strips for which the maximum

twitch heights obtained during the first and third concentration−response curves differed by 10% were used.

**Nociceptive Test.** Male CD-1 mice (Harlan SRC, Milan, Italy), weighing 25−35 g, were used. Animals were kept in a room with a 12:12 h light/dark cycle (lights on at 9:00 a.m.), a temperature of 20−22 °C, and a humidity of 45−55%. They were offered free access to tap water and food pellets (4RF18, Mucedola, Settimo Milanese, Italy). Animal testing was carried out according to the European Community Council Directive of 24 November 1986 (86/609/EEC).

Nociception was evaluated by the radiant heat tail flick test: briefly, it consists of the irradiation of the lower third of the tail with an IR source (Ugo Basile, Comerio, Italy). The basal predrug latency, ranged between 2 and 3 s, was calculated as the mean of two trials performed at 30 min interval. Then mice received **9** (1 mg/kg, sc) or related vehicle (DMSO 1%), 30 min before morphine (5.0 mg/kg, sc) administration or saline. The antinociceptive activity was evaluated 30, 60, 90, and 120 min after morphine injection. A cutoff latency of 12 s was established to minimize tissue damage.

**Statistical Analysis.** Antinociceptive effect was expressed as a percent of the maximum possible effect (MPE) according to the following formula: %MPE = (measured latency−basal latency)/(cutoff time − basal latency) × 100%. Data are reported as means ± SEM. Statistical evaluation of data was carried out by analysis of variance (ANOVA) and sequential differences among means according to Student−Newman−Keuls test. Statistical significance was set at $p < 0.05$.

**Acknowledgment.** We thank the MIUR (Rome), the University of Camerino, the Monti dei Paschi di Siena Foundation, and the Servier for financial support.

**Supporting Information Available:** Elemental analyses for compounds **3**−**10**. This material is available free of charge via the Internet at http://pubs.acs.org.

## References

(1) Martin, W. R.; Eades, C. G.; Thompson, J. A.; Huppler, R. E.; Gilbert, P. E. The effects of morphine- and nalorphine-like drugs in the nondependent and morphine-dependent chronic spinal dog. *J. Pharmacol. Exp. Ther.* **1976**, *197*, 517–532.

(2) Zukin, S. R.; Brady, K. T.; Slifer, B. L.; Balster, R. L. Behavioral and biochemical stereoselectivity of sigma opiate/PCP receptors. *Brain Res.* **1984**, *294*, 174–177.

(3) Quirion, R.; Chicheportiche, R.; Contreras, P. C.; Johnson, K. M.; Lodge, D.; Tam, S. W.; Woods, J. H.; Zukin, S. R. Classification and nomenclature of phencyclidine and sigma receptor sites. *Trends Neurosci.* **1987**, *10*, 444–446.

(4) Quirion, R.; Bowen, W. D.; Itzhak, Y.; Junien, J. L.; Musacchio, J. M.; Rothman, R. B.; Su, T.-P.; Tam, S. W.; Taylor, D. P. A proposal for the classification of sigma binding sites. *Trends Pharmacol. Sci.* **1992**, *13*, 85–86.

(5) Bowen, W. D. Sigma receptors: recent advances and new clinical potentials. *Pharm. Acta Helv.* **2000**, *74*, 211–218.

(6) Su, T.-P.; Junien, J.-L. Sigma receptors in the central nervous system and the periphery. In *Sigma Receptors*; Itzhak, Y., Ed.; Academic Press: London, 1994; pp 21−44.

(7) Walker, J. M.; Bowen, W. D.; Walker, F. O.; Matsumoto, R. R.; de Costa, B.; Rice, K. C. Sigma receptors: biology and function. *Pharmacol. Rev.* **1990**, *42*, 355–402.

(8) Wolfe, S. A., Jr.; De Souza, E. B. Sigma and phencyclidine receptors in the brain-endocrine-immune axis. *NIDA Res. Monogr.* **1993**, *133*, 95–123.

(9) Vilner, B. J.; John, C. S.; Bowen, W. D. Sigma-1 and sigma-2 receptors are expressed in a wide variety of human and rodent tumor cell lines. *Cancer Res.* **1995**, *55*, 408–413.

(10) Hanner, M.; Moebius, F. F.; Flandorfer, A.; Knaus, H.-G.; Striessnig, J.; Kempner, E.; Glossman, H. Purification, molecular cloning, and expression of the mammalian sigma$_1$-binding site. *Proc. Natl. Acad. Sci. U.S.A.* **1996**, *93*, 8072–8077.

(11) Seth, P.; Fei, Y.-J.; Li, H. W.; Huang, W.; Leibach, F. H.; Ganapathy, V. Cloning and functional characterization of a $\sigma$ receptor from rat brain. *J. Neurochem.* **1998**, *70*, 922–931.

(12) Pan, Y.-X.; Mei, J.; Xu, J.; Wan, B.-L.; Zuckerman, A.; Pasternak, G. W. Cloning and characterization of a mouse $\sigma_1$ receptor. *J. Neurochem.* **1998**, *70*, 2279–2285.

(13) Kekuda, R.; Prasad, P. D.; Fei, Y.-J.; Leibach, F. H.; Ganapathy, V. Cloning and functional expression of the human type 1 sigma receptor (hSigmaR1). *Biochem. Biophys. Res. Commun.* **1996**, *229*, 553–558.

(14) Fontanilla, D.; Johannessen, M.; Hajipour, A. R.; Cozzi, N. V.; Jackson, M. B.; Ruoho, A. E. The hallucinogen *N*,*N*-dimethyltryptamine (DMT) is an endogenous sigma-1 receptor regulator. *Science* **2009**, *323*, 934–937.

(15) Connick, J. H.; Hanlon, G.; Roberts, J.; France, L.; Fox, P. K.; Nicholson, C. D. Multiple $\sigma$ binding sites in guinea pig and rat brain membranes: G-protein interactions. *Br. J. Pharmacol.* **1992**, *107*, 726–731.

(16) Hong, W.; Werling, L. L. Evidence that the $\sigma_1$ receptor is not directly coupled to G proteins. *Eur. J. Pharmacol.* **2000**, *408*, 117–125.

(17) Hayashi, T.; Su, T.-P. Sigma-1 receptor chaperones at the ER-mitochondrion interface regulate $Ca^{2+}$ signaling and cell survival. *Cell* **2007**, *131*, 596–610.

(18) Vilner, B. J.; Bowen, W. D. Modulation of cellular calcium by sigma-2 receptors: release from intracellular stores in human SK-N-SH neuroblastoma cells. *J. Pharmacol. Exp. Ther.* **2000**, *292*, 900–911.

(19) Monnet, F. P. Sigma-1 receptor as regulator of neuronal intracellular $Ca^{2+}$: clinical and therapeutic relevance. *Biol. Cell* **2005**, *97*, 873–883.

(20) Aydar, E.; Palmer, C. P.; Djamgoz, M. B. A. Sigma receptors and cancer: possible involvement of ion channels. *Cancer Res.* **2004**, *64*, 5029–5035.

(21) Wilke, R. A.; Lupardus, P. J.; Grandy, D. K.; Rubinstein, M.; Low, M. J.; Jackson, M. B. $K^+$ channel modulation in rodent neurohypophysial nerve terminals by sigma receptors and not by dopamine receptors. *J. Physiol.* **1999**, *517.2*, 391–406.

(22) Bermack, J. E.; Debonnel, G. Distinct modulatory roles of sigma receptor subtypes on glutamatergic responses in the dorsal hippocampus. *Synapse* **2005**, *55*, 37–44.

(23) Gudelsky, G. A. Biphasic effect of sigma receptor ligands on the extracellular concentration of dopamine in the striatum of the rat. *J. Neural Transm.* **1999**, *106*, 849–856.

(24) Matsuno, K.; Matsunaga, K.; Senda, T.; Mita, S. Increase in extracellular acetylcholine level by sigma ligands in rat frontal cortex. *J. Pharmacol. Exp. Ther.* **1993**, *265*, 851–859.

(25) de la Puente, B.; Nadal, X.; Portillo-Salido, E.; Sánchez-Arroyos, R.; Ovalle, S.; Palacios, G.; Muro, A.; Romero, L.; Entrena, J. M.; Baeyens, J. M.; López-García, J. A.; Maldonado, R.; Zamanillo, D.; Vela, J. M. Sigma-1 receptors regulate activity-induced spinal sensitization and neuropathic pain after peripheral nerve injury. *Pain* **2009**, *145*, 294–303.

(26) Skuza, G. Potential antidepressant activity of sigma ligands. *Pol. J. Pharmacol.* **2003**, *55*, 923–934.

(27) Matsumoto, R. R.; Liu, Y.; Lerner, M.; Howard, E. W.; Brackett, D. J. $\sigma$ Receptors: potential medications development target for anti-cocaine agents. *Eur. J. Pharmacol.* **2003**, *469*, 1–12.

(28) Lin, Z.; Kadaba, P. K. Molecular targets for the rational design of antiepileptic drugs and related neuroprotective agents. *Med. Res. Rev.* **1997**, *17*, 537–572.

(29) Rowley, M.; Bristow, L. J.; Hutson, P. H. Current and novel approaches to the drug treatment of schizophrenia. *J. Med. Chem.* **2001**, *44*, 477–501.

(30) Maurice, T.; Lockhart, B. P. Neuroprotective and anti-amnesic potentials of sigma ($\sigma$) receptor ligands. *Prog. Neuro-Psychopharmacol. Biol. Psychiatry* **1997**, *21*, 69–102.

(31) Marrazzo, A.; Caraci, F.; Salinaro, E. T.; Su, T.-P.; Copani, A.; Ronsisvalle, G. Neuroprotective effects of sigma-1 receptor agonists against beta-amyloid-induced toxicity. *NeuroReport* **2005**, *16*, 1223–1226.

(32) Akhter, N.; Shiba, K.; Ogawa, K.; Tsuji, S.; Kinuya, S.; Nakajima, K.; Mori, H. A change of in vivo characteristics depending on specific activity of radioiodinated (+)-2-[4-(4-iodophenyl)piperidino]cyclohexanol [(+)-pIV] as a ligand for sigma receptor imaging. *Nucl. Med. Biol.* **2008**, *35*, 29–34.

(33) Tu, Z.; Xu, J.; Jones, L. A.; Li, S.; Dumstorff, C.; Vangveravong, S.; Chen, D. L.; Wheeler, K. T.; Welch, M. J.; Mach, R. H. Fluorine-18-labeled benzamide analogues for imaging the $\sigma_2$ receptor status of solid tumors with positron emission tomography. *J. Med. Chem.* **2007**, *50*, 3194–3204.

(34) de Costa, B. R.; He, X.-S. Structure−activity relationships and evolution of sigma receptor ligands (1976−present). In *Sigma Receptors*; Itzhak, Y., Ed.; Academic Press: London, 1994; pp 45−111.

(35) Guitart, X.; Codony, X; Monroy, X. Sigma receptors: biology and therapeutic potential. *Psychopharmacology* **2004**, *174*, 301–319.

(36) Chu, W.; Xu, J.; Zhou, D.; Zhang, F.; Jones, L. A.; Wheeler, K. T.; Mach, R. H. New N-substituted 9-azabicyclo[3.3.1]nonan-3α-yl phenylcarbamate analogs as $\sigma_2$ receptor ligands: synthesis, in vitro characterization, and evaluation as PET imaging and chemosensitization agents. *Bioorg. Med. Chem.* **2009**, *17*, 1222–1231.
(37) Glennon, R. A. Pharmacophore identification for sigma-1 ($\sigma_1$) receptor binding: application of the "Deconstruction−Reconstruction−Elaboration" approach. *Mini-Rev. Med. Chem.* **2005**, *5*, 927–940.
(38) Quaglia, W.; Giannella, M.; Piergentili, A.; Pigini, M.; Brasili, L.; Di Toro, R.; Rossetti, L.; Spampinato, S.; Melchiorre, C. 1′-Benzyl-3,4-dihydrospiro[2*H*-1-benzothiopyran-2,4′-piperidine] (Spipethiane), a potent and highly selective $\sigma_1$ ligand. *J. Med. Chem.* **1998**, *41*, 1557–1560.
(39) Uto, Y.; Kiyotsuka, Y. Preparation of spiropiperidine derivatives as stearoyl-CoA-desaturase inhibitors. Patent WO2008/056687, **2008**.
(40) Yamato, M.; Hashigaki, K.; Tsutsumi, A.; Tasaka, K. Synthesis and structure−activity relationship of spiro[isochroman-piperidine] analogs for inhibition of histamine release. *Chem. Pharm. Bull.* **1981**, *29*, 3494–3498.
(41) Gilligan, P. J.; Kergaye, A. A.; Lewis, B. M.; McElroy, J. F. Piperidinyltetralin $\sigma$ ligands. *J. Med. Chem.* **1994**, *37*, 364–370.
(42) Arnoldi, A.; Carughi, M. A simple synthesis of 2-substituted 1-benzothiophenes and 3-substituted 2*H*-1-benzothiopyrans. *Synthesis* **1988**, *2*, 155–157.
(43) Corvaisier, A. Recherche en série hétérocyclique. I.- Synthèse de chalcones, o-hydroxychalcones, chromannones et chromones dérivées d'aldéhydes hétérocycliques. *Bull. Soc. Chim. Fr.* **1962**, 528–535.
(44) Topolski, M. Electrophilic reactions of carbenoids. Synthesis of fused heterocyclic systems via intramolecular nucleophilic substitution of carbenoids. *J. Org. Chem.* **1995**, *60*, 5588–5594.
(45) Naruto, S.; Sugano, Y.; Matsui, Y.; Tonohiro, T.; Kaneko, T.; Iwata, N. Indole and indazole derivatives, for the treatment and prophylaxis of cerebral disorders, their preparation and their use. Patent EP562832, **1993**.
(46) Ganapathy, M. E.; Prasad, P. D.; Huang, W.; Seth, P.; Leibach, F. H.; Ganapathy, V. Molecular and ligand-binding characterization of the $\sigma$-receptor in the Jurkat human T lymphocyte cell line. *J. Pharmacol. Exp. Ther.* **1999**, *289*, 251–260.
(47) Bowen, W. D.; de Costa, B. R.; Hellewell, S. B.; Walker, J. M.; Rice, K. C. [$^3$H]-(+)-pentazocine: a potent and highly selective benzomorphan-based probe for sigma-1 receptors. *Mol. Neuropharmacol.* **1993**, *3*, 117–126.
(48) Azzariti, A.; Colabufo, N. A.; Berardi, F.; Porcelli, L.; Niso, M.; Simone, G. M.; Perrone, R.; Paradiso, A. Cyclohexylpiperazine derivative PB28, a $\sigma_2$ agonist and $\sigma_1$ antagonist receptor, inhibits cell growth, modulates P-glycoprotein, and synergizes with anthracyclines in breast cancer. *Mol. Cancer Ther.* **2006**, *5*, 1807–1816.
(49) Grever, M. R.; Shepartz, S. A.; Chabner, B. A. The National Cancer Institute: cancer drug discovery and development program. *Semin. Oncol.* **1992**, *19*, 622–638.
(50) Vermes, I.; Haanen, C.; Steffens-Nakken, H.; Reutelingsperger, C. A novel assay for apoptosis flow cytometric detection of phosphatidylserine expression on early apoptotic cells using fluorescein labelled Annexin V. *J. Immunol. Methods* **1995**, *184*, 39–51.
(51) Darzynkiewicz, Z.; Juan, G. DNA content measurement for DNA ploidy and cell cycle analysis. *Curr. Protoc. Cytometry* **2001**, 7.5.1–7.5.24.
(52) Campbell, B. G.; Scherz, M. W.; Keana, J. F. W.; Weber, E. Sigma receptors regulate contractions of the guinea pig ileum longitudinal muscle/myenteric plexus preparation elicited by both electrical stimulation and exogenous serotonin. *J. Neurosci.* **1989**, *9*, 3380–3391.
(53) Marrazzo, A.; Parenti, C.; Scavo, V.; Ronsisvalle, S.; Scoto, G. M.; Ronsisvalle, G. In vivo evaluation of (+)-MR200 as a new selective sigma ligand modulating MOP, DOP and KOP supraspinal analgesia. *Life Sci.* **2006**, *78*, 2449–2453.
(54) Mei, J.; Pasternak, G. W. $\sigma_1$ Receptor modulation of opioid analgesia in the mouse. *J. Pharmacol. Exp. Ther.* **2002**, *300*, 1070–1074.
(55) Oberdorf, C.; Schepmann, D.; Vela, J. M.; Diaz, J. L.; Holenz, J.; Wünsch, B. Thiophene bioisosteres of spirocyclic $\sigma$ receptor ligands. 1. N-Substituted spiro[piperidine-4,4′-thieno[3,2-*c*]-pyrans]. *J. Med. Chem.* **2008**, *51*, 6531–6537.
(56) Colabufo, N. A.; Berardi, F.; Contino, M.; Niso, M.; Abate, C.; Perrone, R.; Tortorella, V. Antiproliferative and cytotoxic effects of some $\sigma_2$ agonists and $\sigma_1$ antagonists in tumour cell lines. *Naunyn-Schmiedeberg's Arch. Pharmacol.* **2004**, *370*, 106–113.
(57) Spruce, B. A.; Campbell, L. A.; McTavish, N.; Cooper, M. A.; Appleyard, M. V. L.; O'Neill, M.; Howie, J.; Samson, J.; Watt, S.; Murray, K.; McLean, D.; Leslie, N. R.; Safrany, S. T.; Ferguson, M. J.; Peters, J. A.; Prescott, A. R.; Box, G.; Hayes, A.; Nutley, B.; Raynaund, F.; Downes, C. P.; Lambert, J. J.; Thompson, A. M.; Eccles, S. Small molecule antagonists of the $\sigma$-1 receptor cause selective release of the death program in tumor and self-reliant cells and inhibit tumor growth in vitro and in vivo. *Cancer Res.* **2004**, *64*, 4875–4886.
(58) Renaudo, A.; L'Hoste, S.; Guizouarn, H.; Borgèse, F.; Soriani, O. Cancer cell cycle modulated by a functional coupling between sigma-1 receptors and $Cl^-$ channels. *J. Biol. Chem.* **2007**, *282*, 2259–2267.
(59) Aydar, E.; Onganer, P.; Perret, R.; Djamgoz, M. B.; Palmer, C. P. The expression and functional characterization of sigma ($\sigma$) 1 receptors in breast cancer cell lines. *Cancer Lett.* **2006**, *242*, 245–257.
(60) Levine, A. J. p53, the cellular gatekeeper for growth and division. *Cell* **1997**, *88*, 323–331.
(61) White, E. Life, death, and the pursuit of apoptosis. *Genes Dev.* **1996**, *10*, 1–15.
(62) Chien, C.-C.; Pasternak, G. W. Sigma antagonists potentiate opioid analgesia in rats. *Neurosci. Lett.* **1995**, *190*, 137–139.
(63) Bradford, M. M. A rapid and sensitive method for the quantitation of microgram quantities of protein utilizing the principle of protein-dye binding. *Anal. Biochem.* **1976**, *72*, 248–254.
(64) Cheng, Y. C.; Prusoff, W. H. Relationship between the inhibition constant ($K_i$) and the concentration of inhibitor which causes 50% inhibition ($I_{50}$) of an enzymatic reaction. *Biochem. Pharmacol. Methods* **1985**, *22*, 3099–3108.